

## Article

# Beta-Caryophyllene Induces Significant Changes in the Lipid Bilayer at Room and Physiological Temperatures: ATR-FTIR Spectroscopy Studies

 Ivan D. Yakimov, Ilya M. Kolmogorov and Irina M. Le-Deygen \* 

Department of Chemical Enzymology, Moscow State University, Moscow 119991, Russia; yaki99va@yandex.ru (I.D.Y.); kolmogorov2001@mail.ru (I.M.K.)

\* Correspondence: i.m.deygen@gmail.com

**Abstract:** Beta-caryophyllene (BCP) is a natural bicyclic sesquiterpene with high biological activity. Potentially, it can be used in the treatment of a wide range of neurological diseases. However, to date, there are practically no data on the interaction of BCP with biological membranes. In the present work, we studied for the first time the interaction of BCP with model membranes—liposomes based on egg yolk phosphatidylcholine (Egg PC) with a variable cholesterol content (from 0 to 25 w.%). Using ATR-FTIR spectroscopy, we have shown that the membrane rigidity and cholesterol content dramatically affect the nature of the interaction of BCP with the bilayer both at room temperature and at physiological temperatures. The incorporation of BCP into the thickness of the bilayer leads to changes in the subpolar region of the bilayer, and at a high cholesterol content, it can provoke the formation of defects in the membrane.

**Keywords:** beta-caryophyllene; membranes; liposomes; FTIR



**Citation:** Yakimov, I.D.; Kolmogorov, I.M.; Le-Deygen, I.M. Beta-Caryophyllene Induces Significant Changes in the Lipid Bilayer at Room and Physiological Temperatures: ATR-FTIR Spectroscopy Studies. *Biophysica* **2023**, *3*, 501–512. <https://doi.org/10.3390/biophysica3030033>

Academic Editor: Herbert Schneckenburger

Received: 28 July 2023

Revised: 26 August 2023

Accepted: 28 August 2023

Published: 30 August 2023



**Copyright:** © 2023 by the authors. Licensee MDPI, Basel, Switzerland. This article is an open access article distributed under the terms and conditions of the Creative Commons Attribution (CC BY) license (<https://creativecommons.org/licenses/by/4.0/>).

## 1. Introduction

Beta-caryophyllene is a bicyclic sesquiterpene (Figure 1) found in numerous plants and their essential oils, such as angustifolia lavender, black pepper, cardamom, and clary sage.

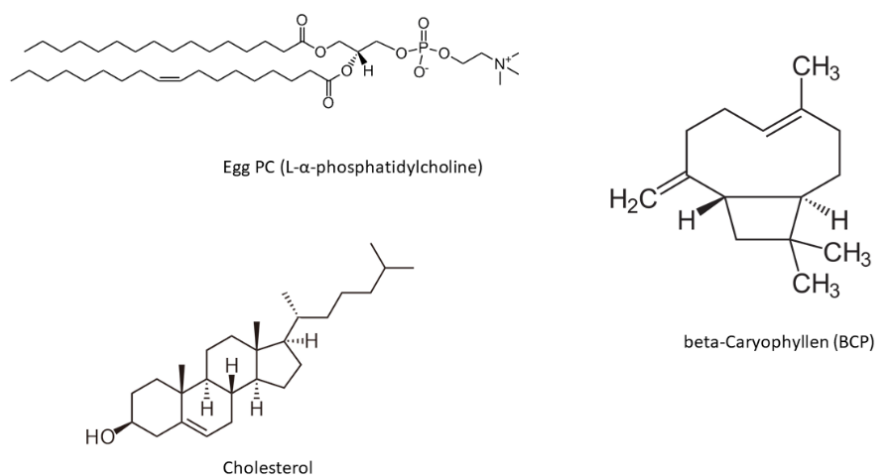


**Figure 1.** Formulae of substances under consideration.

Several types of biological activity of beta-caryophyllene (BCP) are known, including antimicrobial, antileishmanial, antimalarial, local anesthetic, antispasmodic, and anticonvulsant activity [1]. However, BCP attracts attention to the greatest extent for its anti-inflammatory [2], antiseptic properties [3]. Recently, BCP activity has been demonstrated in the treatment of diseases of the nervous system, including Parkinson's disease [4], and multiple sclerosis [5], atherosclerosis [6], and tumors [7].

BCP is a selective agonist of the CB2 receptor, which is a therapeutic target for the treatment of inflammation, pain, atherosclerosis, colitis, cerebral ischemia, and inflammation of the brain [8]. Since BCP does not show activity to CB1 (cannabinoid type 1 receptor), it does not cause psychotropic effects and distortion of consciousness. These facts make beta-caryophyllene a potential analgesic and analogue of opiates, which are prescribed for persistent chronic pain syndromes [9].

Beta-caryophyllene desensitizes chemo-resistant cancer cells when used with anti-cancer drugs [2]. It has been found to be able to be included in target signaling pathways involved in inflammation and cancer, including the HMGB1/TLR4 and STAT3 signaling pathways [7].

Probably, the biological effect of BCP is largely due to its interaction with cell membranes, but at present there is no consistent study of the physicochemical mechanisms of this process. Obviously, the interaction of a phospholipid membrane with a large sesquiterpene molecule can significantly depend on the rigidity of the membrane; therefore, it seems appropriate to study the interaction of BCP with a liquid crystal membrane, for example, based on egg yolk phosphatidylcholine, with different rigidity due to the variable cholesterol content.

In this work, we aimed to analyze the interaction of BCP with model lipid membranes—liposomes based on egg lecithin, and also containing 10 and 25 w.% of cholesterol. It is known from the literature that liposomes based on egg lecithin are in the liquid crystalline phase, and cholesterol provides the membrane rigidity [10,11]. The role of cholesterol as a potential binding site as well as the influence of the membrane rigidity on the interaction between BCP and bilayer are obscure. One of the tasks of the current work was to discover the main functional groups of lipids capable of binding BCP, as well as to reveal the role of membrane rigidity by means of comparing different lipid composition. Since the behavior of lipid bilayers is highly dependent on temperature, for more detailed information, we investigated the behavior of systems at temperatures from 22 to 40 °C to take into account the influence of physiological temperatures.

## 2. Materials and Methods

### 2.1. Materials

Egg yolk phosphatidylcholine (Egg PC) and cholesterol (Chol) were obtained from Avanti Polar Lipids (Alabaster, AL, USA). Sodium phosphate buffer tablets for solution preparation were obtained from Pan-Eco (Moscow, Russia).  $\text{CHCl}_3$  was obtained from Reakhim (Moscow, Russia).  $\beta$ -caryophyllene was obtained from Givaudan (New York, NY, USA).

### 2.2. Liposome Preparation

Liposomes were obtained by lipid film hydration followed by sonication according to the previously published protocol [12]. Solutions of Egg PC and Chol in chloroform (25 mg/mL) in the required mass ratio of 75:25 or 90:10 or Egg PC (monocomponent vesicles) with total lipid mass of 10 mg were placed in a round-bottom flask; the solvent was then removed on a rotary evaporator at a temperature below 55 °C. The resulting thin film was dispersed with 8  $\mu\text{L}$  of beta-caryophyllene and 0.01 M sodium phosphate buffer solution (pH = 7.4) to a lipid concentration of 5 mg/mL; the flask was then exposed to an ultrasonic bath (37 Hz) for 5 min. The opaque suspension was transferred into a plastic tube and sonicated (22 kHz) for 10 min continuously with constant cooling on a 4710 Cole-Parmer Instrument disperser (Vernon Hills, IL, USA).

### 2.3. DLS Measurements

Determination of the hydrodynamic diameter and  $\zeta$ -potential of vesicles was carried out using a Zetasizer Nano S Malvern (Malvern, UK) (4 mW He-Ne laser, 633 nm) in a thermostatted cell at 22 °C. The software Malvern S Zetasizer Nano 4.2 Software 37 Zeta (Malvern, UK) was used to analyze autocorrelation curves.

#### 2.4. ATR-FTIR Spectroscopy

The spectra were recorded using a Bruker Tensor 27 ATR-FTIR spectrometer (Ettlingen, Germany) equipped with an MCT detector cooled with liquid nitrogen and Huber thermostat (Offenburg, Germany). The measurements were carried out in a BioATR II thermostated cell (Bruker, Ettlingen, Germany) using a single reflection ZnSe element at 22 °C and continuous purging of the system with dry air using a compressor (JUN-AIR, Redditch, UK). An aliquot (50 µL) of the corresponding solution was applied to the internal reflection element, and the spectrum was recorded three times in the range from 3000 to 900 cm<sup>-1</sup> with a resolution of 1 cm<sup>-1</sup>; 70-fold scanning and averaging were performed. The background spectrum was registered in the same way and was automatically subtracted by the software. The spectra were analyzed using Opus 8.6 software, Bruker. When recording the ATR-FTIR spectra of liposomes loaded with BCP, a portion of β-caryophyllene in equal concentration was used as a background solution. For phase transition studies, the temperature was controlled with a Huber thermostat in the range from 22 °C up to 42 °C. For each temperature, background spectra were recorded.

Carbonyl group spectral region deconvolution was conducted as described [13]. Curve-fitting was performed using the Bruker Opus 7.5 software. The center positions of the band components were found by the second-derivative production as 1728 and 1743 cm<sup>-1</sup>. Bands were fitted by components of Gauss shape, with a correlation of at least 0.995.

### 3. Results and Discussion

#### 3.1. Interaction between Liposomal Membrane and BCP at Room Temperature

BCP contains only a hydrophobic moiety (Figure 1) and according to the PubChem database, logP is 6.3, indicating almost total water-insolubility. Thus, for BCP-loaded liposomes, one could expect that BCP is located in the hydrophobic area of the membrane without any interaction with polar functional groups. To disclose the mechanism of interaction between bilayer and BCP, we obtained 3 types of vesicles with variable proportions of Egg PC and Chol.

It is well-known that liposomes composed on Egg PC are in a liquid-crystalline state both at room and at physiological temperatures [14]. On the other hand, according to [15], adding cholesterol allows more organized and rigid bilayers. The inclusion of cholesterol in the composition of vesicles also leads to a higher Young's modulus for liposomes: e.g., Egg PC vesicles are about 1.97 ± 0.75 µPa, while for Egg PC:Chol 85:15, this value is 12.07 ± 1.53 µPa [16]. We therefore investigated whether the rigidity of the membrane will depend on the nature of the interaction of the BCP with the bilayer at temperature and with changes in temperature.

According to the DLS data, all samples were about 100–120 nm in diameter and possessed almost neutral ζ-potential (Table 1).

**Table 1.** Hydrodynamic diameter (D<sub>h</sub>) and ζ-potential of control and BCP-loaded liposomes based on Egg PC and Chol in various combinations; 0.01 M sodium phosphate buffer solution, pH = 7.4, T = 22 °C. Mean ± SD (n = 3).

Lipid Composition	D <sub>h</sub> , nm (Z-Average)	ζ-Potential, mV
Egg PC control	106 ± 4	2.2 ± 1.2
Egg PC + BCP	108 ± 8	3.7 ± 1.0
Egg PC:Chol 90:10 liposomes	112 ± 3	6.6 ± 2.4
Egg PC:Chol 90:10 liposomes + BCP	110 ± 6	2.0 ± 0.6
Egg PC:Chol 75:25 liposomes	114 ± 4	3.3 ± 1.4
Egg PC:Chol 75:25 liposomes + BCP	116 ± 5	4.1 ± 2.0

To discover the mechanism of interaction between membrane and BCP, one could use ATR-FTIR spectroscopy as a powerful method for thorough study of the heterogeneous colloids such as liposomal suspension providing detailed information on the state of functional groups of lipids. On the ATR-FTIR spectrum of liposomes (Figure 2), several informative

bands are presented. The most intensive bands in the high-wavenumber area correspond to the symmetrical ( $\nu\text{CH}_2$  s,  $2850 \pm 3 \text{ cm}^{-1}$ ) and asymmetrical ( $\nu\text{CH}_2$  as,  $2919 \pm 6 \text{ cm}^{-1}$ ) stretching oscillation of the  $\text{CH}_2$  group. Changes in this area are usually caused by re-arrangement in the hydrophobic part of the bilayer, such as phase transitions [17] or interactions with large hydrophobic moieties in ligands [12].

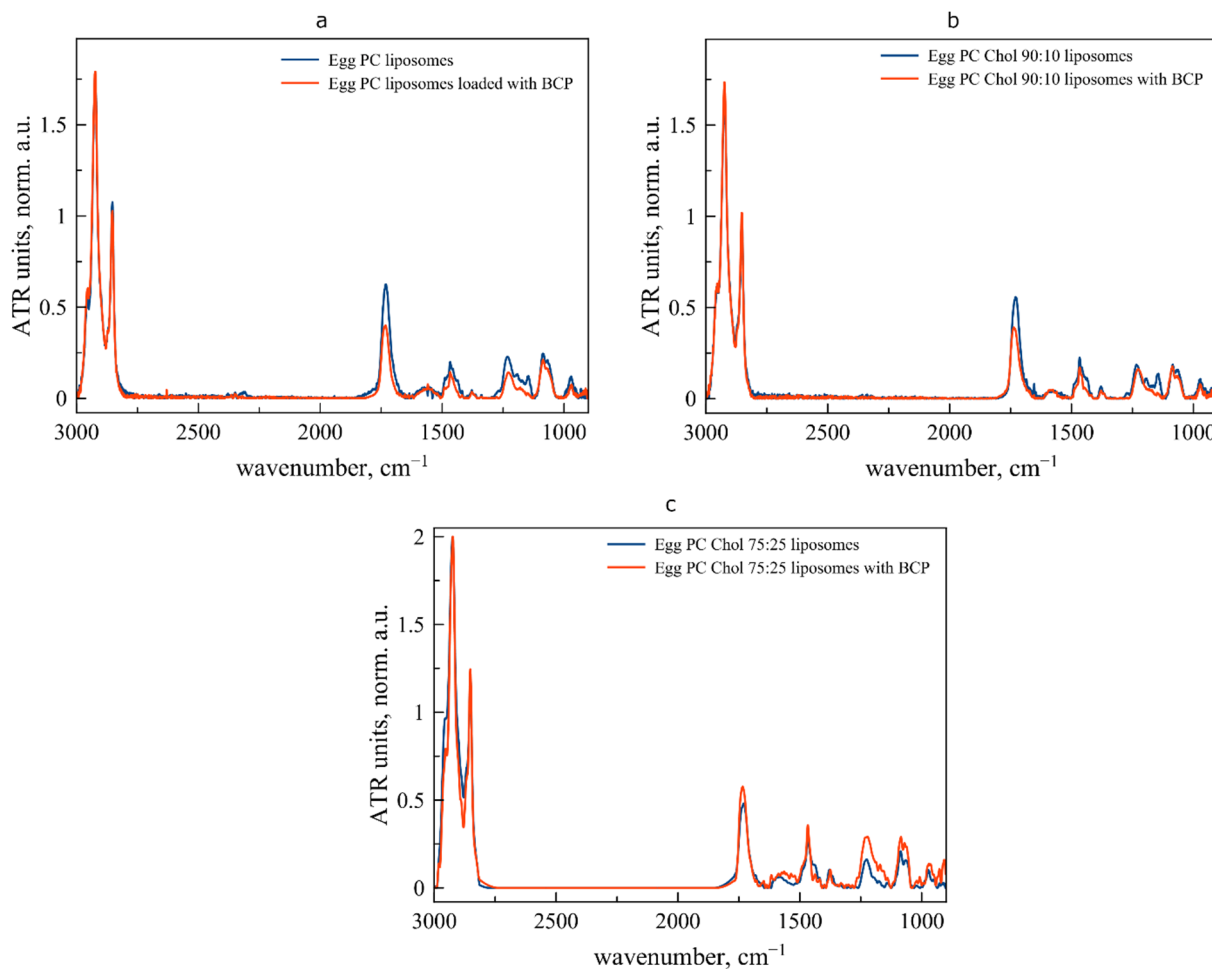


**Figure 2.** Normalized ATR-FTIR spectra of liposomes of various lipid compositions: (a) Egg PC, (b) Egg PC:Chol 90:10, (c) Egg PC:Chol 75:25: control (blue lines) and loaded with BCP (red lines). Total lipid concentration 5 mg/mL; 0.01 M Na phosphate-buffered solution, pH = 7.4, T = 22 °C.

A carbonyl group valence oscillation band is located in the area of  $1715\text{--}1750 \text{ cm}^{-1}$  [18]. It is very sensitive to the changes in the microenvironment on the lipid–water surface. This band is especially interesting because it usually consists of 2–3 components corresponding to different degrees of hydration of carbonyl groups [19]. Thus, highly hydrated groups are characterized by absorption in the region of lower wave numbers, while poorly hydrated groups, for example, those involved in the formation of hydrogen bonds with ligands, are characterized by absorption in the region of high wave numbers. The decomposition of the absorption band of the carbonyl group makes it possible to more accurately follow the redistribution of these groups over the degrees of hydration and track subtle changes in the bilayer.

In the binding of polar ligands, a special role is played by the phosphate group, which is characterized by two absorption bands  $\nu\text{PO}_2^-$  s  $1088 \text{ cm}^{-1}$  and  $\nu\text{PO}_2^-$  as  $1250\text{--}1220 \text{ cm}^{-1}$ . Of particular interest is the absorption band of asymmetric stretching vibrations  $\nu\text{PO}_2^-$  as, which undergoes a high-frequency shift when bound to a cationic ligand, such as an amino group [17,20].

Positions of the main absorption bands on the spectra of control and BCP-loaded liposomes are presented in Table 2. The binding of BCP already at room temperature significantly affects the bilayer. Firstly, comparing data for control and BCP-loaded vesicles, one can observe that the absorption band  $\nu\text{CH}_2$  as in all cases undergoes a low-frequency shift, indicating a decrease in the mobility of hydrophobic chains in the membrane. This is an expected effect, which is apparently associated with the penetration of a large BCP molecule into the bilayer. This effect is most pronounced for monocomponent vesicles that do not contain cholesterol additives.

**Table 2.** Position of the main absorption bands ( $\text{cm}^{-1}$ ) in the ATR-FTIR spectra of liposomes and liposomal form of  $\beta$ -caryophyllene (BCP); 0.01 M sodium phosphate buffer solution, pH 7.4, T = 22 °C. Mean  $\pm$  SD ( $n = 3$ ).

Sample	$\nu\text{CH}_2$ as	$\nu\text{CH}_2$ s	$\nu\text{CO}$	$\nu\text{PO}_2^-$ as
Egg PC liposomes	2923.1 $\pm$ 0.2	2852.6 $\pm$ 0.5	1731.3 $\pm$ 0.2	1231.9 $\pm$ 0.2
Egg PC liposomes + BCP	2922.6 $\pm$ 0.2	2853.0 $\pm$ 0.5	1732.1 $\pm$ 0.2 1736.0 shoulder	1228.7 $\pm$ 0.2
Egg PC:Chol 90:10 liposomes	2923.6 $\pm$ 0.2	2852.6 $\pm$ 0.5	1730.0 $\pm$ 0.2	1233.8 $\pm$ 0.2
Egg PC:Chol 90:10 liposomes + BCP	2922.8 $\pm$ 0.2	2852.4 $\pm$ 0.5	1736.5 $\pm$ 0.2 1732.0 shoulder	1227.1 $\pm$ 0.2
Egg PC:Chol 75:25 liposomes	2924.4 $\pm$ 0.2	2851.8 $\pm$ 0.5	1729.9 $\pm$ 0.2 1740.0 shoulder	1226.0 $\pm$ 0.2
Egg PC:Chol 75:25 liposomes + BCP	2923.7 $\pm$ 0.2	2851.8 $\pm$ 0.5	1734.7 $\pm$ 0.2	1225.5 $\pm$ 0.2

An interesting pattern is observed for the absorption band of the carbonyl group. For liposomes Egg PC loaded with BCP, the main peak  $\nu\text{CO}$  remains with a stable position at ca. 1731  $\text{cm}^{-1}$  and a shoulder appears at 1736  $\text{cm}^{-1}$ , which is characteristic of carbonyl groups with a lower degree of hydration [11]. Due to the fact that it typically manifests when the membrane interacts with polar ligands, the presence of a low-hydrated component may be unexpected. The hydration shell is disrupted by the creation of hydrogen bonds with the ligand, which causes the absorption band to shift to the area with high wave numbers. BCP cannot directly interact with lipid carbonyl groups due to the structure. However, the packing density of acyl chains increases when a large hydrophobic molecule is incorporated into the bilayer, as shown by changes in the relevant spectral area  $\nu\text{CH}_2$  as. Thus, the degree of hydration of CO may formally decrease as a result of these perturbations, which have the potential to destabilize the hydration shell.

We used a curve-fitting approach (Figure 3, Table 3) for the carbonyl group's absorption band to quantify this behavior [18,19]. The primary model, which corresponds to high- and low-hydrated groups, is a two-component one based on 1728 and 1743  $\text{cm}^{-1}$ . We observed a considerable rise in the integral ratio of the component of low-hydrated carbonyl groups when comparing the calculations for control Egg PC and loaded liposomes (Figure 3a,b, Table 2). This impact becomes even greater for liposomes containing 10% by mass cholesterol. Indicating the heterogeneity of the circumpolar area of the bilayer, the primary band (1730  $\text{cm}^{-1}$ ) shifts to the region with higher wavenumbers (1736.5  $\text{cm}^{-1}$ ) while a shoulder stays in place (1730  $\text{cm}^{-1}$ ). This effect becomes considerably more pronounced when the cholesterol concentration approaches 25%. A population of low-hydrated carbonyl groups is evident even in unbound liposomes (ca. 25%), most likely related to the domains that are rich in cholesterol [21]. BCP's presence in the bilayer causes the highest amount of low-hydrated carbonyl groups (almost 40%) to be there.

What determines the decrease in carbonyl group hydration is the subsequent issue. This is frequently related to the formation of hydrogen bonds with polar ligands, such as polycations or molecules of polar drugs; nevertheless, the BCP structure lacks any suitable groups, and the level of lipophilicity in the molecule strongly suggests that the molecule is most likely located in the hydrophobic thickness of the bilayer. Since it is well-known that phosphate groups are located on the surface of the vesicles, it follows that the disturbance of the hydration shell of carbonyl groups and the expulsion of some water

molecules from the circumpolar area should have an impact on the phosphate groups. Monocomponent, “liquid” liposomes (Egg PC) reveal this phenomenon of decreasing the degree of hydration for the  $\nu\text{PO}_2^-$  as absorption bands with the highest strength. This process is shown by the particular shift of the peak from 1231.9 to 1228.7  $\text{cm}^{-1}$ . Evidently, the more rigid the membrane, the more challenging it is to maintain hydration-related water on the surface of the vesicles; thus, such an effect cannot be observed for liposomes containing 25% cholesterol.

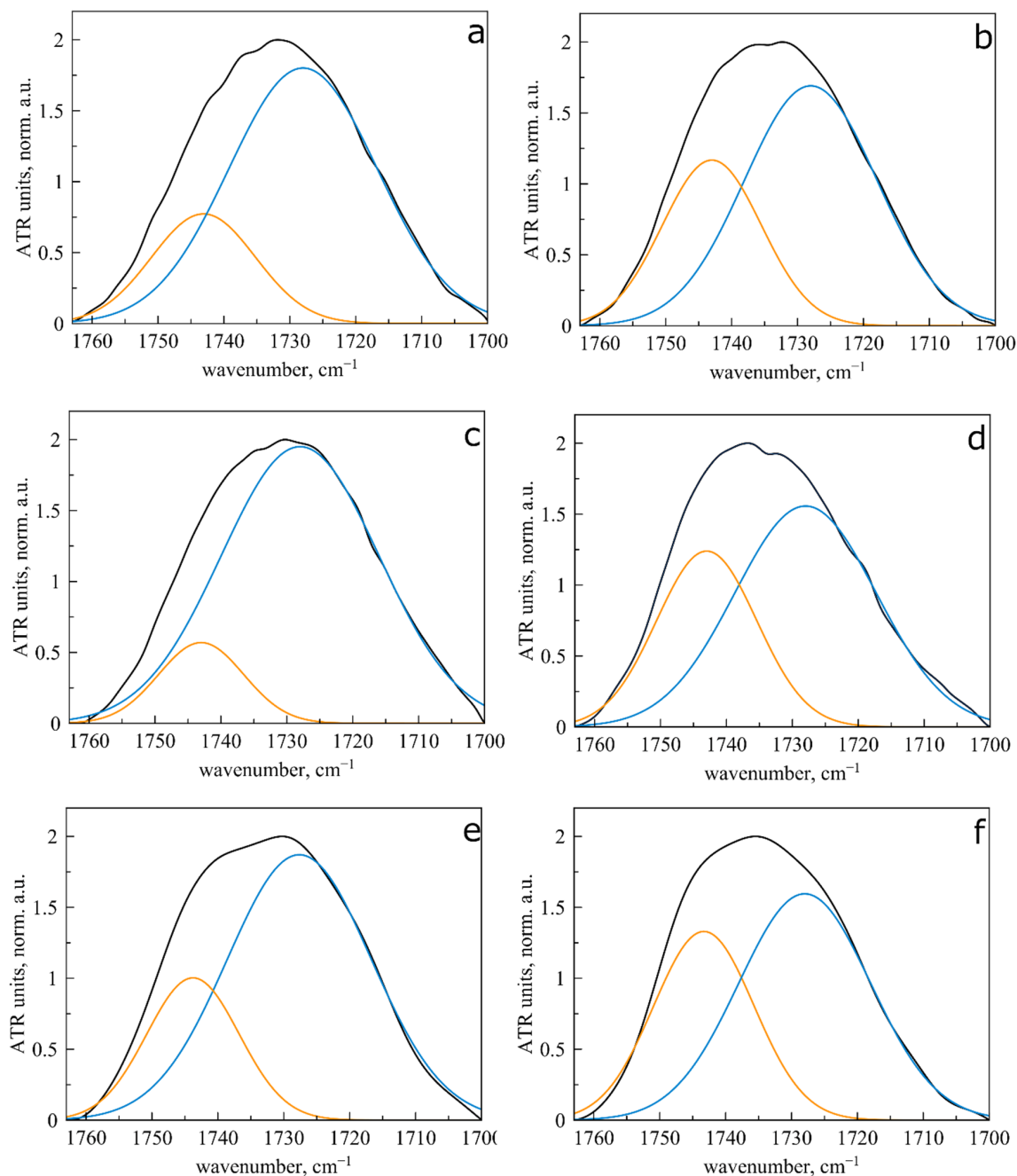


**Figure 3.** ATR-FTIR spectra of liposomes and liposomal forms of BCP: carbonyl group area. Deconvolution was conducted with Gaussians. The black line is the initial spectrum, orange—component of low-hydrated carbonyl groups, blue—component of medium-hydrated carbonyl groups. (a) Egg PC liposomes. (b) Egg PC liposomes + BCP. (c) Egg PC:Chol 90:10 liposomes. (d) Egg PC:Chol 90:10 + BCP liposomes. (e) Egg PC:Chol 75:25 liposomes (f) Egg PC:Chol 75:25 liposomes + BCP; 0.01 M sodium-phosphate-buffered solution pH = 7.4, T = 22 °C.

**Table 3.** Integral share of carbonyl groups components; 0.01 M sodium phosphate-buffered solution, pH = 7.4, T = 22 °C. Mean  $\pm$  SD ( $n = 3$ ).

Sample	1728 $\text{cm}^{-1}$ (High Hydrated), Integral Share, %	1743 $\text{cm}^{-1}$ (Low Hydrated), Integral Share, %
Egg PC liposomes	77 $\pm$ 2	23 $\pm$ 2
Egg PC liposomes + BCP	66 $\pm$ 2	34 $\pm$ 2
Egg PC:Chol 90:10 liposomes	86 $\pm$ 2	14 $\pm$ 2
Egg PC:Chol 90:10 liposomes + BCP	64 $\pm$ 2	36 $\pm$ 2
Egg PC:Chol 75:25 liposomes	74 $\pm$ 2	26 $\pm$ 2
Egg PC:Chol 75:25 liposomes + BCP	61 $\pm$ 2	39 $\pm$ 2

As a result, the data obtained by ATR-FTIR spectroscopy clearly demonstrate that the interaction of BCP with the membrane is more complex than just simple integration into the hydrophobic area of the bilayer. Both the circumpolar region of the membrane and the surface undergo alterations. However, the behavior of membranes may change significantly when shifting from room to physiological temperature, which may have an important influence on the interaction between bilayer and BCP. Here we consider the way these three systems with variable lipid composition behave in the 22 to 40 °C temperature range.

### 3.2. Behavior of Liposomal Forms of BCP during the Transition from Room to Physiological Temperature

At room temperature, Egg PC liposomes are in the liquid crystalline phase, also called the liquid-disordered (Ld) or La phase [22], which is associated with great mobility of hydrophobic chains. For example, lateral diffusion rates vary from  $10^7$  to  $10^8 \text{ cm}^2\text{s}^{-1}$  [23]. Temperature of phase transition (“melting temperature”) for Egg PC is around (−10)–(−5) °C [24].

In the presence of cholesterol, the most typical phase for Egg PC-based vesicles is liquid-ordered phase (Lo) or Lb phase [22]. Chol molecules, located in the bilayer, form interactions between hydroxy groups and the polar head groups of Egg PC, resulting in lower mobility of the acyl chains in this region of the membrane.

As Egg PC liposomes are already in Ld phase, they do not undergo any significant changes upon heating up to 40 °C (Figure 4a). In contrast, BCP-loaded Egg PC vesicles demonstrate firstly accelerated “melting” up to 30 °C, followed by reproducible minimum. These changes indicate an interaction of BCP with the bilayer.

For liposomes containing 10 w.% of cholesterol (Figure 4b, grey line), the shape of the curve becomes more complicated. Probably, the appearance of minima and maxima is associated with rearrangements in the membrane. The shape of the curve for liposomes loaded with BCP is similar to the control one (Figure 4b, red line); however, in the region from 28 to 35 °C, the process slows down. The slowing effect is even more pronounced for liposomes containing 25 w.% of cholesterol. This membrane is already much more rigid, and when heated, the mobility of acyl chains evenly increases from 26 to 40 °C (Figure 4c, grey line). Turning on the BCP leads to blocking of this process: first, the mobility of the chains is significantly reduced (Figure 4c, red line) followed by a return to the initial peak position.

As a result of the above, vesicles with a high cholesterol content have a particularly dramatic reaction to BCP’s effect on the phase transition. We performed the deconvolution of the carbonyl group’s absorption band for each sample in the temperature range of 22 °C to 40 °C in order to better understand the processes taking place during the phase transition. We monitored an increase in the integral share of the 1743  $\text{cm}^{-1}$  component corresponding to low-hydrated groups ( $\psi_{\text{LH}}$ ) as we kept the two-component model. When BCP was added to liposomes, the fraction of this component increased for all lipid compositions at room temperature (Table 3). We now analyze the dynamics of this value  $\psi_{\text{LH}}$  throughout the phase transition.

For monocomponent vesicles Egg PC, both for the control and loaded, the changes in  $\psi_{LH}$  with increasing temperature are insignificant (Figure 5a), which, together with the data on the change in the  $\nu_{CH_2}$  as the peak position, indicates only a minor rearrangement of the bilayer. Probably, a slight heating allows the BCP to penetrate better into the hydrophobic thickness of the bilayer.

A completely different pattern is observed for liposomes Egg PC:Chol 75:25. The course of the thermogram for unloaded liposomes indicates a significant increase in the mobility of acyl chains (Figure 4c, grey line). This process is accompanied by a significant decrease in the proportion of low-hydrated carbonyl groups (Figure 5c, grey line), which is in good agreement with previously published data [25]. Indeed, as the membrane becomes more fluid, carbonyl groups become more accessible to water molecules, which increases their degree of hydration.

For BCP-loaded liposomes Egg PC:Chol 75:25, the atypical course of the thermogram (Figure 4c, red line) is confirmed by significant changes in the degree of hydration of carbonyl groups (Figure 5c, red line). A sharp decrease in the mobility of hydrophobic chains in the area of 28–32 °C is accompanied by a decrease in the integral share of low-hydrated carbonyl groups  $\psi_{LH}$ , thus, formally, the degree of hydration of the circumpolar area is increasing. Such an effect can be observed during the formation of defects in the membrane [26], when the search for the optimal position of the BCP in a sufficiently rigid bilayer leads to a violation of the integrity of the membrane.

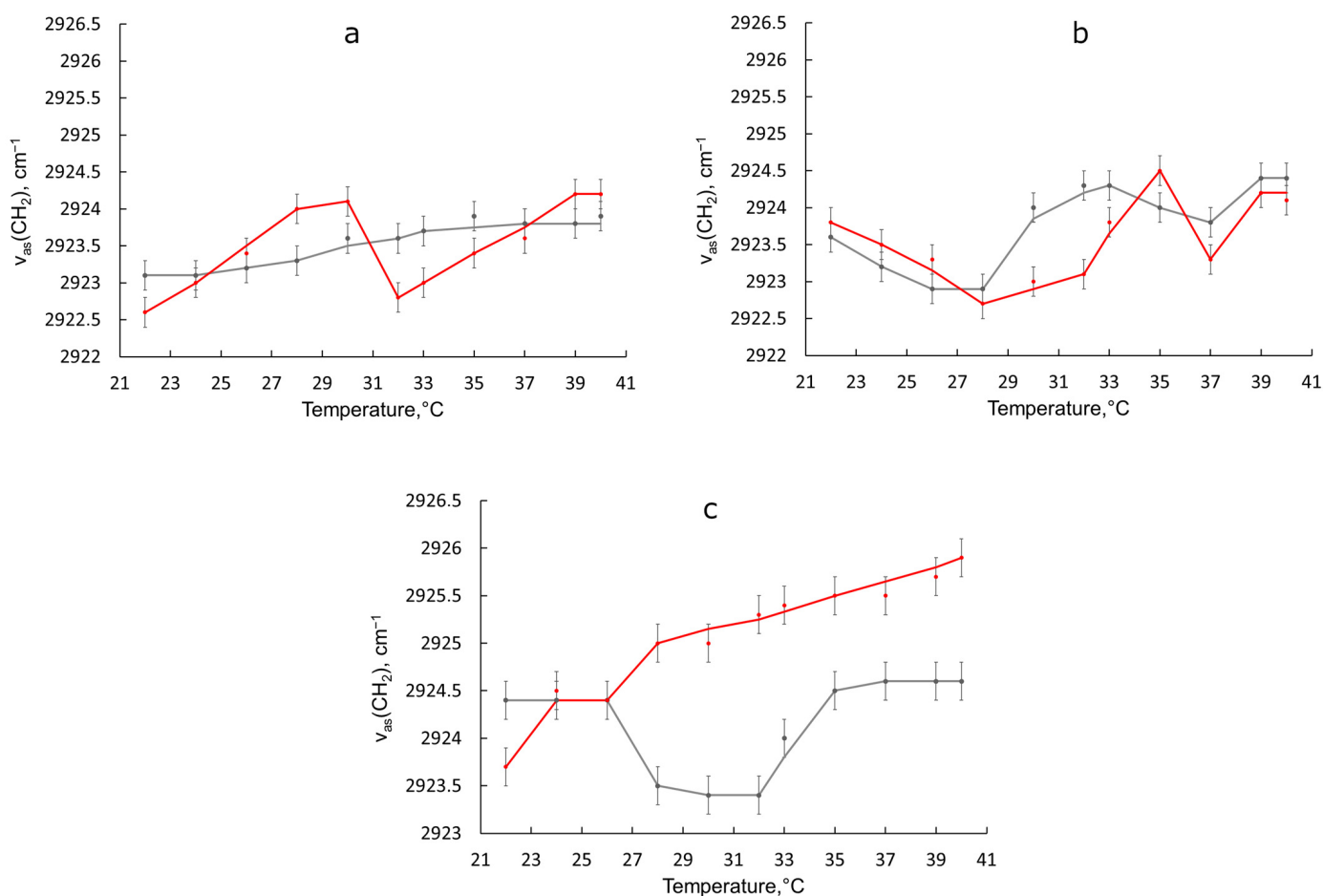


**Figure 4.** Dependence on temperature of  $\nu_{CH_2}$  as peak position for (a) Egg PC, (b) Egg PC:Chol 90:10, (c) Egg PC:Chol 75:25. For all figures, data for unloaded liposomes are presented in grey and for BCP-loaded are presented in red. For each point, the SD ( $n = 3$ ) is presented. Total lipid concentration 5 mg/mL, 0.02 M PBS, pH = 7.4.

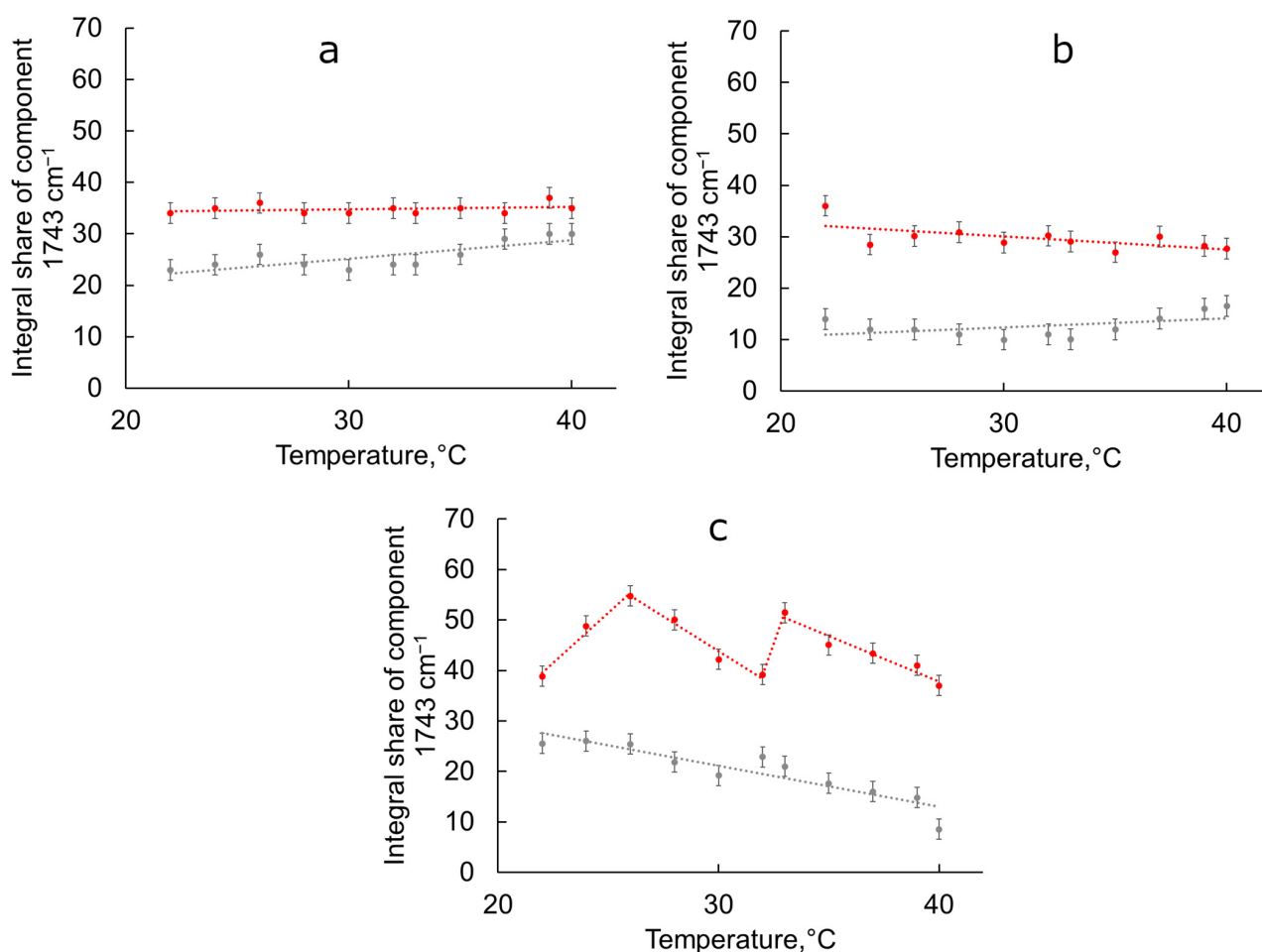


**Figure 5.** Dependence of the integral share of the component  $1743\text{ cm}^{-1}$  in the  $\nu\text{CO}$  band, corresponding to the low-hydrated state of carbonyl groups  $\psi_{\text{LH}}$  on temperature for (a) Egg PC, (b) Egg PC:Chol 90:10, (c) Egg PC:Chol 75:25. For all figures, data for unloaded liposomes are presented in grey and for BCP-loaded are presented in red. For each point, the SD ( $n = 3$ ) is presented. Total lipid concentration  $5\text{ mg/mL}$ ,  $0.02\text{ M PBS pH} = 7.4$ .

For liposomes containing 10% cholesterol, a similar pattern is observed (Figure 5b). The state of carbonyl groups upon heating from  $22\text{ }^{\circ}\text{C}$  to  $40\text{ }^{\circ}\text{C}$  remains practically unchanged for both control and loaded vesicles. Thus, the observed perturbations in the mobility of hydrophobic chains on the thermogram of loaded vesicles (Figure 4b red line) are associated with changes only in the hydrophobic area of the bilayer and do not even involve the circumpolar region.

### 3.3. The Effect of Lipid Composition on the Interaction of BCP with Liposomal Bilayers

The data obtained indicate the decisive role of cholesterol in the interaction of BCP with liposomes based on Egg PC.

Recently, the role of cholesterol in the interaction between drugs and lipid bilayers was examined with molecular dynamics (MD) simulations, for example, for ibuprofen and fully hydrated 1,2-dimyristoyl-sn-glycero-3-phosphocholine (DMPC) bilayer with variable mass ratio of cholesterol (0, 16, and 36 w.%) [27]. The authors concluded that 36 w.% of Chol in the bilayer leads to a higher free energy barrier and decreases the translocation of the ibuprofen through the bilayer. Kremkow and coauthors reported that ibuprofen indeed disturbs the acyl chains package and increased the mobility of the lipid head groups [10].

Here we have clearly demonstrated that another molecule—BCP—influences the microenvironment of functional groups of lipids already at room temperature, while upon

heating, the most pronounced changes are observed for the most rigid membrane with 25 w.% of Chol.

Unlike BCP, ibuprofen is a small molecule, in the structure of which there is one polar functional group—a carboxyl group. BCP, in contrast, is a completely hydrophobic terpene hydrocarbon that does not contain any moieties capable of interacting with the polar groups of lipids. However, considering the experimental data, its effect on the hydrophobic thickness of the bilayer is so significant that it causes perturbations in the subpolar and polar regions of the membrane.

For all lipid compositions at room temperature, BCP is incorporated into the hydrophobic thickness of the bilayer. Carbonyl and phosphate groups, representing circumpolar and polar areas of bilayer, become redistributed over the degrees of hydration due to disturbances in the packing of hydrophobic chains and perturbations in the membrane. With increasing temperature, systems Egg PC and Egg PC:Chol 90:10 remain stable, retaining the liquid crystal phase. In contrast, loaded vesicles Egg PC:Chol 75:25 undergo significant changes both in the thickness of the bilayer and in the circumpolar region. A decrease in the mobility of hydrophobic chains, coupled with a decrease in the integral fraction of low-hydrated carbonyl groups, indicates the potential formation of defects in the membrane. Given that the proportion of cholesterol in a eukaryotic cell reaches 30% [28], the observed effect may play an important role in the study of the biological activity of BCP.

#### 4. Conclusions

In this work, we studied the interaction of the terpene hydrocarbon BCP, which has a wide spectrum of biological activity, with PC-based liposomes with variable cholesterol content. It has been established that BCP is located in the hydrophobic part of the bilayer and causes significant perturbations in the membrane, leading to a decrease in the degree of hydration of lipid carbonyl groups. The effect becomes more pronounced with an increase in cholesterol content. Main features of the interaction are presented in Table 4.

**Table 4.** Main features of the interaction BCP—PC bilayer with variable content of Chol; 0.01 M sodium phosphate-buffered solution, pH = 7.4, T = 22 °C.

Lipid Composition	Main Features of Interaction, RT	Main Features of Interaction upon Heating
Egg PC	Strong interaction with hydrophobic area + weak interaction with circumpolar area	Almost unchanged pattern of interaction
Egg PC:Chol 90:10	Strong interaction with hydrophobic and circumpolar area	Almost unchanged pattern of interaction
Egg PC:Chol 75:25 liposomes	Strong interaction with hydrophobic and circumpolar area	Probably: formation of defects in bilayer in the temperature range 28–32 °C

When heated from 22 to 40 °C, the systems without cholesterol and with 10 w.% remain practically unchanged, while for the Egg PC:Chol 75:25 vesicles, dramatic changes are observed both in the hydrophobic region and in the circumpolar region. The deconvolution of the absorption band of the carbonyl group made it possible to trace that in the temperature range 28–32 °C, there is a clear decrease in the integral share of low-hydrated carbonyl groups, which, together with a decrease in the mobility of hydrophobic chains, may indicate the formation of defects in the membrane. The results obtained shed light on the mechanisms of BCP interaction with biological membranes and may be useful in studying the chemical basis of the biological activity of BCP.

**Author Contributions:** Conceptualization, I.M.L.-D.; methodology, I.M.L.-D. and I.M.K.; validation, I.M.L.-D., I.D.Y. and I.M.K.; formal analysis, I.M.L.-D., I.D.Y. and I.M.K.; investigation, I.D.Y. and I.M.K.; resources, I.M.L.-D.; data curation, I.M.L.-D., I.D.Y. and I.M.K.; writing—original draft preparation, I.M.L.-D.; writing—review and editing, I.D.Y. and I.M.K.; visualization, I.M.L.-D. and I.D.Y.; supervision, I.M.L.-D.; project administration, I.M.L.-D. All authors have read and agreed to the published version of the manuscript.

**Funding:** This research was funded by the President of Russia grant for young PhDs 075-15-2022-397 (lipid purchase).

**Data Availability Statement:** The data presented in this study are available on request from the corresponding author. The data are not publicly available due to privacy reasons.

**Acknowledgments:** The work was performed using the equipment (FTIR spectrometer Bruker Tensor 27) of the program for the development of Moscow State University and equipment purchased by the Developmental Program of Lomonosov Moscow State University (PNR 5.13).

**Conflicts of Interest:** The authors declare no conflict of interest.

## References

1. Fidyk, K.; Fiedorowicz, A.; Strzdała, L.; Szumny, A.  $\beta$ -caryophyllene and  $\beta$ -caryophyllene oxide—Natural compounds of anticancer and analgesic properties. *Cancer Med.* **2016**, *5*, 3007–3017. [[CrossRef](#)]
2. Di Giacomo, S.; Di Sotto, A.; Mazzanti, G.; Wink, M. Chemosensitizing properties of  $\beta$ -caryophyllene and  $\beta$ -caryophyllene oxide in combination with doxorubicin in human cancer cells. *Anticancer Res.* **2017**, *37*, 1191–1196. [[PubMed](#)]
3. Orchard, A.; Van Vuuren, S. Commercial Essential Oils as Potential Antimicrobials to Treat Skin Diseases. *Evid.-Based Complement. Altern. Med.* **2017**, *2017*, 4517971. [[CrossRef](#)] [[PubMed](#)]
4. Ojha, S.; Javed, H.; Azimullah, S.; Haque, M.E.  $\beta$ -Caryophyllene, a phytocannabinoid attenuates oxidative stress, neuroinflammation, glial activation, and salvages dopaminergic neurons in a rat model of Parkinson disease. *Mol. Cell. Biochem.* **2016**, *418*, 59–70. [[CrossRef](#)] [[PubMed](#)]
5. Alberti, T.B.; Barbosa, W.L.R.; Vieira, J.L.F.; Raposo, N.R.B.; Dutra, R.C. (–)- $\beta$ -caryophyllene, a CB2 receptor-selective phytocannabinoid, suppresses motor paralysis and neuroinflammation in a murine model of multiple sclerosis. *Int. J. Mol. Sci.* **2017**, *18*, 691. [[CrossRef](#)] [[PubMed](#)]
6. Baldissera, M.D.; Souza, C.F.; Grando, T.H.; Stefani, L.M.; Monteiro, S.G.  $\beta$ -caryophyllene reduces atherogenic index and coronary risk index in hypercholesterolemic rats: The involvement of cardiac oxidative damage. *Chem. Biol. Interact.* **2017**, *270*, 9–14. [[CrossRef](#)] [[PubMed](#)]
7. Mannino, F.; Pallio, G.; Corsaro, R.; Minutoli, L.; Altavilla, D.; Vermiglio, G.; Allegra, A.; Eid, A.H.; Bitto, A.; Squadrito, F.; et al. Beta-caryophyllene exhibits anti-proliferative effects through apoptosis induction and cell cycle modulation in multiple myeloma cells. *Cancers* **2021**, *13*, 5741. [[CrossRef](#)]
8. Di Sotto, A.; Paolicelli, P.; Nardoni, M.; Abete, L.; Garzoli, S.; Di Giacomo, S.; Mazzanti, G.; Casadei, M.A.; Petralito, S. SPC liposomes as possible delivery systems for improving bioavailability of the natural sesquiterpene  $\beta$ -caryophyllene: Lamellarity and drug-loading as key features for a rational drug delivery design. *Pharmaceutics* **2018**, *10*, 274. [[CrossRef](#)]
9. Ceccarelli, I.; Fiorenzani, P.; Pessina, F.; Pinassi, J.; Aglianò, M.; Miragliotta, V.; Aloisi, A.M. The CB2 Agonist  $\beta$ -Caryophyllene in Male and Female Rats Exposed to a Model of Persistent Inflammatory Pain. *Front. Neurosci.* **2020**, *14*, 850. [[CrossRef](#)]
10. Kremkow, J.; Luck, M.; Huster, D.; Müller, P.; Scheidt, H.A. Membrane interaction of ibuprofen with cholesterol-containing lipid membranes. *Biomolecules* **2020**, *10*, 1384. [[CrossRef](#)]
11. Arsov, Z.; Quaroni, L. Direct interaction between cholesterol and phosphatidylcholines in hydrated membranes revealed by ATR-FTIR spectroscopy. *Chem. Phys. Lipids* **2007**, *150*, 35–48. [[CrossRef](#)] [[PubMed](#)]
12. Le-Deygen, I.M.; Safronova, A.S.; Mamaeva, P.V.; Kolmogorov, I.M.; Skuredina, A.A.; Kudryashova, E.V. Drug–Membrane Interaction as Revealed by Spectroscopic Methods: The Role of Drug Structure in the Example of Rifampicin, Levofloxacin and Rapamycin. *Biophysica* **2022**, *2*, 353–365. [[CrossRef](#)]
13. Le-Deygen, I.M.; Safronova, A.S.; Mamaeva, P.V.; Skuredina, A.A.; Kudryashova, E.V. Cholesterol Significantly Affects the Interactions between Pirfenidone and DPPC Liposomes: Spectroscopic Studies. *Biophysica* **2022**, *2*, 79–88. [[CrossRef](#)]
14. Taylor, K.M.G.; Morris, R.M. Thermal analysis of phase transition behaviour in liposomes. *Thermochim. Acta* **1995**, *248*, 289–301. [[CrossRef](#)]
15. Liu, D.Z.; Chen, W.Y.; Tasi, L.M.; Yang, S.P. Microcalorimetric and shear studies on the effects of cholesterol on the physical stability of lipid vesicles. *Colloids Surf. A Physicochem. Eng. Asp.* **2000**, *172*, 57–67. [[CrossRef](#)]
16. Liang, X.; Mao, G.; Ng, K.Y.S. Mechanical properties and stability measurement of cholesterol-containing liposome on mica by atomic force microscopy. *J. Colloid. Interface Sci.* **2004**, *278*, 53–62. [[CrossRef](#)]
17. Manrique-Moreno, M.; Moreno, M.M.; Garidel, P.; Suwalsky, M.; Howe, J.; Brandenburg, K. The membrane-activity of Ibuprofen, Diclofenac, and Naproxen: A physico-chemical study with lecithin phospholipids. *Biochim. Biophys. Acta* **2009**, *1788*, 1296–1303. [[CrossRef](#)]
18. Disalvo, E.A.; Frias, M.A. Water state and carbonyl distribution populations in confined regions of lipid bilayers observed by FTIR spectroscopy. *Langmuir* **2013**, *29*, 6969–6974. [[CrossRef](#)]
19. Lewis, R.N.; McElhaney, R.N.; Pohle, W.; Mantsch, H.H. Components of the carbonyl stretching band in the infrared spectra of hydrated 1,2-diacylglycerolipid bilayers: A reevaluation. *Biophys. J.* **1994**, *67*, 2367–2375. [[CrossRef](#)]
20. Deygen, I.M.; Seidl, C.; Kolmel, D.K.; Bednarek, C.; Heissler, S.; Kudryashova, E.V.; Braese, S. Novel Prodrug of Doxorubicin Modified by Stearoylspermine encapsulated into PEG-Chitosan-Stabilized Liposomes. *Langmuir* **2016**, *32*, 10861–10869. [[CrossRef](#)]

21. Coderch, L.; Fonollosa, J.; De Pera, M.; Estelrich, J.; De, A.; Maza, L.; Parra, J.L. Influence of cholesterol on liposome fluidity by EPR Relationship with percutaneous absorption. *J. Control. Release* **2000**, *68*, 85–95. [[CrossRef](#)]
22. Barba-Bon, A.; Nilam, M.; Hennig, A. Supramolecular Chemistry in the Biomembrane. *ChemBioChem* **2020**, *21*, 886–910. [[CrossRef](#)]
23. Korklach, J.; Schwille, P.; Webb, W.W.; Feigenson, G.W. Characterization of lipid bilayer phases by confocal microscopy and fluorescence correlation spectroscopy. *Proc. Natl. Acad. Sci. USA* **1999**, *96*, 8461–8466. [[CrossRef](#)] [[PubMed](#)]
24. Grandois, J.L.E.; Marchioni, E.; Minjie Zhao, F.G.; Ennahar, S.; Bindler, F. investigation of natural phosphatidylcholine sources: Separation and identification by liquid chromatography-electrospray ionization-tandem mass spectrometry (lc-esi-ms2) of molecular species. *J. Agric. Food Chem.* **2009**, *57*, 6014–6020. [[CrossRef](#)]
25. Le-Deygen, I.M.; Vlasova, K.Y.; Kutsenok, E.O.; Usvaliev, A.D.; Efremova, M.V.; Zhigachev, A.O.; Rudakovskaya, P.G.; Golovin, D.Y.; Gribovsky, S.L.; Kudryashova, E.V.; et al. Magnetic nanorods for remote disruption of lipid membranes by non-heating low frequency magnetic field. *Nanomedicine* **2019**, *21*, 102065. [[CrossRef](#)] [[PubMed](#)]
26. Yaroslavov, A.A.; Sybachin, A.V.; Zaborova, O.V.; Orlov, V.N.; Ballauff, M.; Talmon, Y.; Menger, F.M. Lipid segregation in membranes of anionic liposomes adsorbed onto polycationic brushes. *Chem.-A Eur. J.* **2013**, *19*, 13674–13678. [[CrossRef](#)] [[PubMed](#)]
27. Khajeh, A.; Modarress, H. The influence of cholesterol on interactions and dynamics of ibuprofen in a lipid bilayer. *Biochim. Biophys. Acta Biomembr.* **2014**, *1838*, 2431–2438. [[CrossRef](#)]
28. Zhang, Y.; Zhang, J.; Li, Q.; Wu, Y.; Wang, D.; Xu, L.; Zhang, Y.; Wang, S.; Wang, T.; Liu, F.; et al. Cholesterol content in cell membrane maintains surface levels of ErbB2 and confers a therapeutic vulnerability in ErbB2-positive breast cancer. *Cell Commun. Signal.* **2019**, *17*, 15. [[CrossRef](#)]

**Disclaimer/Publisher’s Note:** The statements, opinions and data contained in all publications are solely those of the individual author(s) and contributor(s) and not of MDPI and/or the editor(s). MDPI and/or the editor(s) disclaim responsibility for any injury to people or property resulting from any ideas, methods, instructions or products referred to in the content.